ChemPubSoc Europe

DOI: 10.1002/chem.201501854

CHEMISTRY A European Journal Full Paper

Separation Methods |*Hot Paper*|

D_{3h}-Symmetric Porphyrin-Based Rigid Macrocyclic Ligands for Multicofacial Multinuclear Complexes in a One-Nanometer-Sized Cavity

Yohei Ohkoda, Akane Asaishi, Tomoya Namiki, Tomoaki Hashimoto, Midori Yamada, Koichiro Shirai, Yuta Katagami, Tomoaki Sugaya, Makoto Tadokoro,* and Akiharu Satake*[a]

Abstract: The one-step synthesis of D_{3h}-symmetric cyclic porphyrin trimers **1** composed of three 2,2′-[4,4′-bis(methoxycarbonyl)]bipyridyl moieties and three porphyrinatozinc moieties was achieved from a nickel-mediated reductive coupling of *meso*-5,15-bis(6-chloro-4-methoxycarbonylpyrid-2-yl)porphyrinatozinc. Although cyclic trimers **1** were obtained as a mixture that included other cyclic and acyclic porphyrin oligomers, an extremely specific separation was observed only for cyclic trimers **1** when using columns of silica gel modified with pyrenylethyl, cyanopropyl, and other groups. Structural analysis of cyclic trimers **1** was carried out by means of NMR spectroscopy and X-ray crystallography. Treatment of an η^3-allylpalladium complex with a cyclic trimer gave a tris(palladium) complex containing three η^3-allylpalladium groups inside the space, which indicated that the bipyridyl moieties inside the ring could work as bidentate metalloligands.

Introduction

Metal-catalyzed reactions and molecular transformations in nanometer-sized cavities[1] are attracting attention in organic synthesis as biomimetic artificial enzymes and metalloenzymes, in which selective reactions are expected to proceed under ambient conditions. Bi-[2] and multimetallic[2a,3] catalysts and their related di-[4] and multinuclear[5] metal complexes are also attracting attention because of their high potential for selective transformations and multiredox reactions to activate and transform unreactive and inert molecules and chemical bonds. Therefore, their combined study, that is, the construction of multimetallic systems with nanometer-sized cavities, is a challenging target for the next generation of biomimetic and environmentally benign catalysts in organic synthesis.

Macrocyclic[6] and pseudomacrocyclic[7] multidentate ligands, in which all of the coordination sites are directed toward the center of the macrocycle, are potential candidates for cofacial dinuclear and multicofacial multinuclear complexes in which the metal ions work to manipulate a guest molecule cooperatively. Appropriate spaces to accept desired molecules in macrocycles with their rigid skeletons are required to construct such a reaction field. Macrocyclic porphyrin oligomers are candidates that can serve as multinuclear coordination sites within their rigid skeletons.[8] Macrocyclic porphyrin oligomers are interesting materials for photochemical and electronic organic devices,[9] as well as in the field of molecular recognition,[10] selective reactions,[1a,10b] and in ion-transport materials because of their nanometer-sized rigid pores.[11] Synthetic strategies for the production of covalently linked cyclic porphyrin oligomers involve either macrocyclization of appropriately long acyclic porphyrin oligomers prepared by multistep synthesis,[10e,12] or a one-step synthesis from single or multiple porphyrin units by coupling reactions in the presence or absence of templates.[13] In both of these synthetic approaches, separation of the target cyclic porphyrin oligomer from a mixture that contains other cyclic oligomers and acyclic oligomers is a laborious step that can lead to reduced yield. Gel permeation chromatography (GPC) is a common method used to isolate macrocyclic compounds from mixtures. In general, cyclic compounds tend to be eluted later from the GPC column than the corresponding acyclic compounds because the hydrodynamic volumes of cyclic compounds are smaller than those of linear compounds.[12b,c,14] However, the difference is generally small. Therefore, a long column length and/or repeated chromatographic runs are often necessary to isolate the target cyclic oligomer from the mixture.

We have designed new D_{3h}-symmetric macrocyclic ligands **1** for, at most, hexanuclear multicofacial metal complexes (Figure 1). The ligands of **1** are composed of three 2,2′-bipyridyl moieties and three porphyrinato moieties and, in total, six metal ions can be accepted by the three bidentate ligands and the three tetradentate ligands. To increase the solubility of

[a] *Y. Ohkoda, A. Asaishi, T. Namiki, T. Hashimoto, M. Yamada, K. Shirai, Y. Katagami, Dr. T. Sugaya, Prof. M. Tadokoro, Prof. A. Satake*
Graduate School of Chemical Sciences and Technology
Tokyo University of Science, 1-3 Kagurazaka
Shinjuku-ku, Tokyo 162-8601 (Japan)
E-mail: tadokoro@rs.kagu.tus.ac.jp
satake@rs.kagu.tus.ac.jp

Supporting information for this article is available on the WWW under http://dx.doi.org/10.1002/chem.201501854.

multinuclear complexes, and also for further functionalization outside the macrocyclic ligands, we planned to introduce six carboxylic ester groups on the 4,4′-positions of each 2,2′-bipyridyl moiety. Because an orthogonal conformation between each porphyrin moiety and the 2,2′-bipyridyl group is predicted, the three porphyrin groups are expected to arrange themselves to produce a three-dimensional prism-shaped inner space. On the *meso* positions of the three porphyrins, a substituent group (denoted by R in Figure 1) can be introduced during the synthesis of the porphyrin parts. This can be used to control the size of the mouth to the inner space, as well as the size of the inner space. In this study, mesityl (Mes) and ethyl substituents were examined as a bulky aryl group and a small alkyl group, respectively, denoted by **1a** and **1b** in Figure 1.

We planned to achieve the one-step synthesis of **1** by a nickel-mediated reductive coupling reaction of bis[2-(6-chloropyridyl)]porphyrinatozinc **2** (Scheme 1). The reaction led to the formation of a mixture composed of the target cyclic trimer (C-3mer) and other cyclic and acyclic porphyrin oligomers. During the isolation of the C-3mer from the complex mixture, specific retention phenomena were observed by chromatographic analysis with various modified columns of silica gel. Herein, we report on this unusual separation behavior, as well as the efficient isolation of C-3mer **1**, and that the C-3mer has the potential to form versatile macrocyclic ligands for multicofacial multinuclear complexes.

Results and Discussion

Synthesis and isolation of the C-3mer

Porphyrins **2a** and **2b** were synthesized as follows. The corresponding Mes- or ethyl-substituted dipyrromethanes (**3a** and **3b**) and 6-chloro-4-methoxycarbonylpyridyl-2-paraldehyde (**4**) were condensed in the presence of trifluoroacetic acid, followed by oxidation with *p*-chloranil to give the free-base porphyrins **5a** and **5b** in 31 and 25% yield, respectively. Incorporation of zinc(II) ions into the free-base porphyrins gave **2a** and **2b** quantitatively (Scheme S1 in the Supporting Information). Referring to our previous conditions for the synthesis of bis(porphyrins) connected through 2,2′-bpy,[15] nickel-mediated

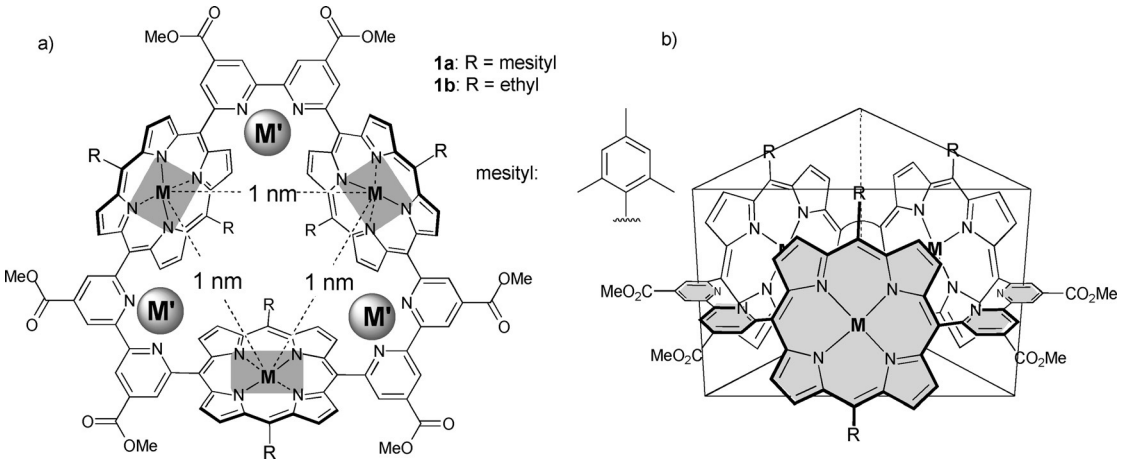

Figure 1. The design of macrocyclic ligand **1** (C-3mer) composed of three 4,4′-methoxycarbonyl-2,2′-bipyridine and three porphyrin groups: a) top view, b) side view. The three 2,2′-bipyridine parts are expected to give metal complexes inside the ring, as shown with gray spheres in a). The six carboxylic acid derivatives outside the ring are expected to increase solubility in various solvent systems. A triangular prism with a triangular space (ca. 1 nm each side) is expected in the orthogonal conformation, as shown in b).

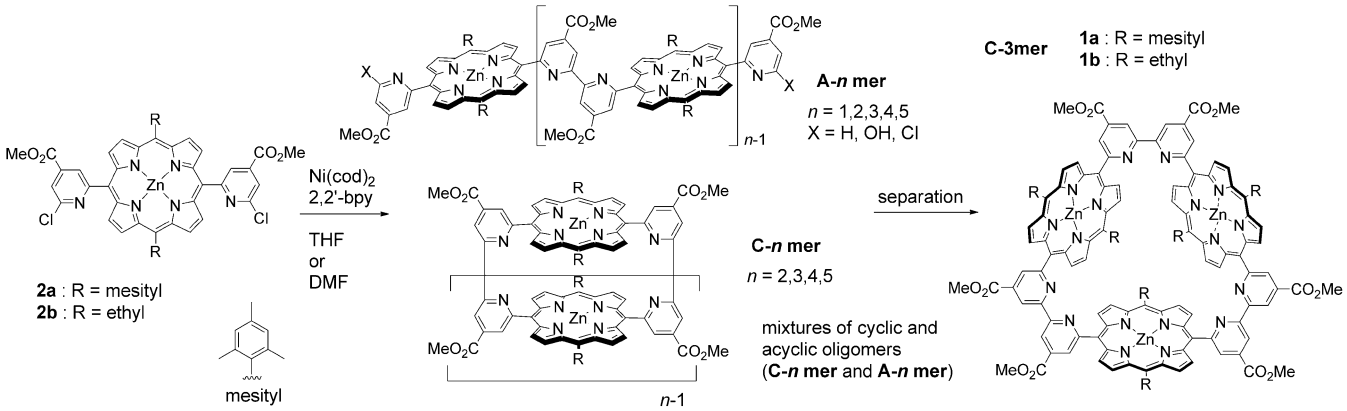

Scheme 1. Synthetic scheme for the preparation of cyclic trimers (C-3mer) **1a** and **1b**; COD = 1,5-cyclooctadiene; 2,2′-bpy = 2,2′-bipyridine.

reductive coupling of **2** was performed. Under these conditions, zinc porphyrins and carboxylic ester moieties in the substrates did not interfere with the reaction. A 1:1 mixture of $[Ni(cod)_2]$ (7–20 equiv) and 2,2′-bpy (7–20 equiv) was treated with porphyrinatozinc **2** in anhydrous THF or anhydrous DMF under an argon atmosphere at 50 °C for 12 h. When ethyl-substituted **2b** was used as the starting material, the coupling reaction proceeded in THF, and seven equivalents of the Ni^0–bpy system were enough to consume most of the starting material. However, in the case of the Mes-substituted complex **2a**, the conditions discussed above were insufficient, and treatment with 20 equivalents of the Ni^0–bpy system in the more active solvent DMF[16] gave better results with regard to the reproducible consumption of starting materials. After the reactions were completed, the mixture was washed with an aqueous ammonium solution to remove excess of nickel species, and the organic layer was extracted with $CHCl_3$. The organic layer was analyzed by means of a GPC system fitted with three polystyrene-based GPC columns (two TSKgel $G2500H_{HR}$ (exclusion limit 20000 Da, 7.8 mm inner diameter (I.D.)×30 cm) and a TSKgel $G2000H_{HR}$ (exclusion limit 10000 Da, 7.8 mm I.D.× 30 cm)) connected in series to a photodiode array detector. The elution profiles from the GPC column monitored at $\lambda =$ 556 and 566 nm, respectively, are depicted as solid lines in Figure 2. Only porphyrin derivatives can be observed at this detection frequency. The plain Gaussian curves shown in Figure 2, which were obtained by deconvolution analysis by using OriginPro8 software, revealed that more than 10 components containing porphyrin oligomers were present in the crude samples. The ratio of each component varied in each experiment, even under the same conditions, and the represented profiles are most typical. In the sample analyzed in Figure 2a and b, the component eluting at 22.5 and 25.6 mL, respectively (shaded areas, assigned as C-3mer, see below), were obtained as the dominant species. The crude mixture was further separated by using a preparative GPC column packed with polystyrene-based gel (Biorad S-X1 (exclusion limit 14000 Da), 3 cm diameter×1 m length) with a mixture of toluene and pyridine (85:15 v/v) as the eluent under atmospheric pressure. MALDI-TOF MS analysis of the fractions showed mass fragments that were approximately two to five times larger than those of starting monomers **2**, which suggested that the reductive coupling reaction produced di- to pentameric porphyrin oligomers. Some estimated structures are shown in Scheme 1. The terminal moieties of acyclic porphyrin oligomers, indicated as X in A-*n*mer in Scheme 1, were assigned as H, Cl, or OH, but some unidentified signals were also observed in the MALDI-TOF MS analyses.

The following detailed analysis describes the case of using ethyl-substituted **2b** as a starting material for the coupling reaction. In the GPC chromatographic separation, compounds corresponding to the trimer were detected in two fractions, with the later eluting compound assigned as the target C-3mer **1b** based on high-resolution MALDI-TOF MS analysis. However, in addition to the target C-3mer **1b**, the fraction contained other mono- and dimeric porphyrin derivatives; thus further purification was required. Although a recycling GPC method could be used to isolate the C-3mer **1b**, other chromatographic techniques involving modified silica gel were surveyed to find a more efficient method. Four analytes, compound **2b** and three fractions containing mainly acyclic dimer (ethyl A-2mer), acyclic trimer (ethyl A-3mer), and cyclic trimer (ethyl C-3mer), were prepared to compare the elution behavior in various modified silica-based columns. Eight HPLC columns (COSMOSIL® series), C18-MS-II, Cholester, PYE, πNAP, NPE, PBB-R, NPE, and CN-MS (4.6 mm I.D.×15 cm), supplied by Nacalai Tesque were tested. The chemical structures of the functional groups on these columns are shown in Figure 3. Thus, octadecyl, cholesterol ether, pyrenylethyl, naphthylethyl, pentabromobenzyl ether, nitrophenylethyl, and cyanopropyl moieties were attached to silica gel (5 μm particle, 120 Å pore). GPC and MALDI-TOF MS analyses of the four analytes used herein are shown in Figures S1–S4 in the Supporting Information. A mixture of toluene and pyridine was used as the eluent. The polarity parameters of the solvents were 2.3 (toluene) and 5.3 (pyridine);[17] therefore, the combination of these solvents worked

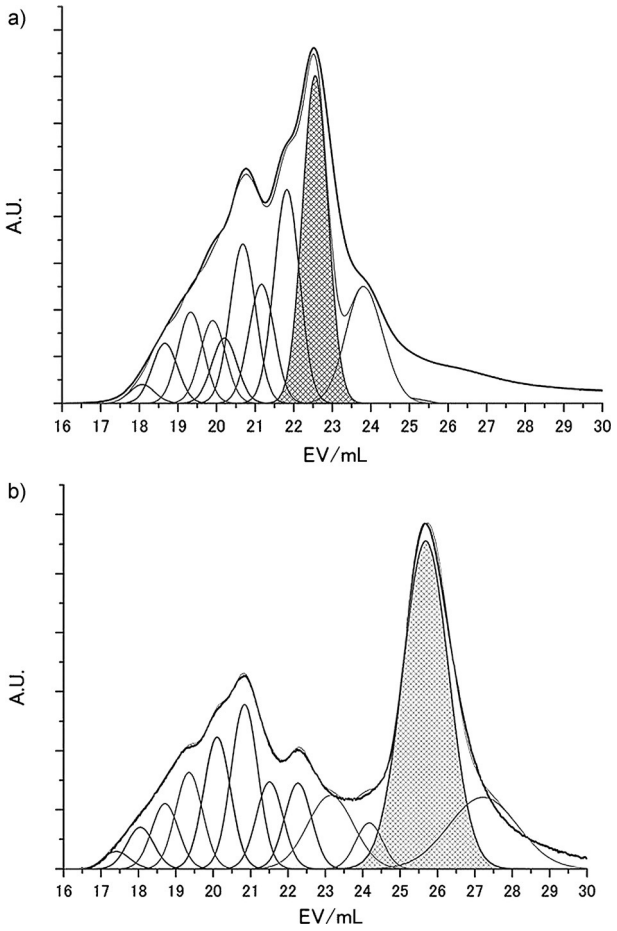

Figure 2. Bold lines in a) and b): typical GPC chromatograms of reaction mixtures obtained by nickel-mediated coupling of **1a** (R = Mes) and **1b** (R = ethyl) (column: TOSOH TSKgel G2500HHR (300 mm (length))×2 (exclusion limit, 20000 Da) + TOSOH TSKgel G2000HHR (300 mm (length))×1 (exclusion limit, 10000 Da), eluent: pyridine, flow rate: 1.0–1.2 mL min^{-1}), monitored at: a) $\lambda = 556$, and b) 566 nm). EV: elution volume. Plain lines in a) and b): deconvolution analysis of the chromatograms by Gaussian curve fitting by means of OriginPro8 software. The shaded peaks indicate C-3mers: a) **1a**, and b) **1b**.

Packing Materials	Bonded Phase Structures
C_{18}-MS-II	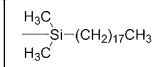
Cholester	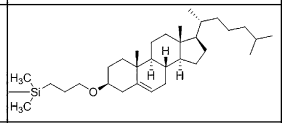
PYE	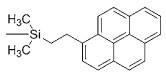
πNAP	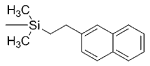
PBB-R	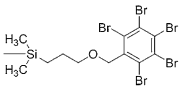
NPE	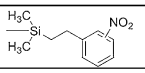
CN-MS	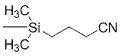

Figure 3. Chemical structures of functional groups bonded to silica gel in modified silica gel columns.

well to elute all of the analytes without adsorption in the stationary phase.

Chromatograms of the analytes obtained by column chromatography with CN-MS as the stationary phase are shown in Figure 4a–d; as a reference, a chromatogram of chloroform (10 μL) is also illustrated in Figure 4e . The peak at 3.88 min in each chromatogram in Figure 4a–d is a shock peak of chloroform used for dilution of the analytes. Peaks of compound **2b**, A-2mer, and A-3mer eluted earlier than the shock peak, which suggested that almost no retention occurred under these conditions, with the A-3mer eluting earliest. In contrast, the C-3mer eluted much later (13.4 min) than those peaks, and impurities contained in this analyte eluted earlier (3–11 min) than the C-3mer. These results indicated the specific interaction of C-3mer with silica gel modified by cyanopropyl groups.

If we assume that the A-3mer was not retained on the CN-MS column at all, then the retention time of this compound could be defined as t_0. Retention factors, $k=(t-t_0)/t_0$, can be calculated based on t_0, as shown for Run 1 in Table 1. Here, $k_{\mathbf{2b}}$, k_{CHCl_3} and $k_{\text{C-3mer }\mathbf{1b}}$ are the retention factors of compounds **2b**, $CHCl_3$, and C-3mer **1b**, respectively. If a retention factor (k) is larger than one, the retention time of the analyte is more than two times longer than that of A-3mer. The large difference in the retention times of A-3mer and C-3mer is noteworthy. Other chromatograms obtained when using C18-MS-II, Cholester, PYE, πNAP, PBB-R, and NPE columns are shown in Figures S5–S7 in the Supporting Information. In the case of C18-MS-II and Cholester, C-3mer **1b** was not retained as well as **2b**, A-2mer, and A-3mer (Figure S5 in the Supporting Information). In contrast, specific retention of C-3mer **1b** was observed in PYE, πNAP, NPE, and PBB-R columns (Figures S6 and S7 in the Supporting Information). In all of the chromatograms, A-3mer eluted first and the retention times of A-3mer can be defined as t_0. Retention factors, k, are listed in Table 1. The retention factors of C-3mer in C18-MS-II and Cholester were 0.04 and 0.02, respectively, which were similar to those of porphyrinatozinc **2b** and C-3mer **1b** and suggested that no interaction was observed between C-3mer **1b** and the stationary phase in C18-MS-II and Cholester. The retention factors of C-3mer **1b** in PYE, πNAP, and PBB-R were in the range 0.88–1.68, whereas that of **2b** remained below 0.1, which indicated that a specific interaction between C-3mer **1b** and the stationary phase was observed.

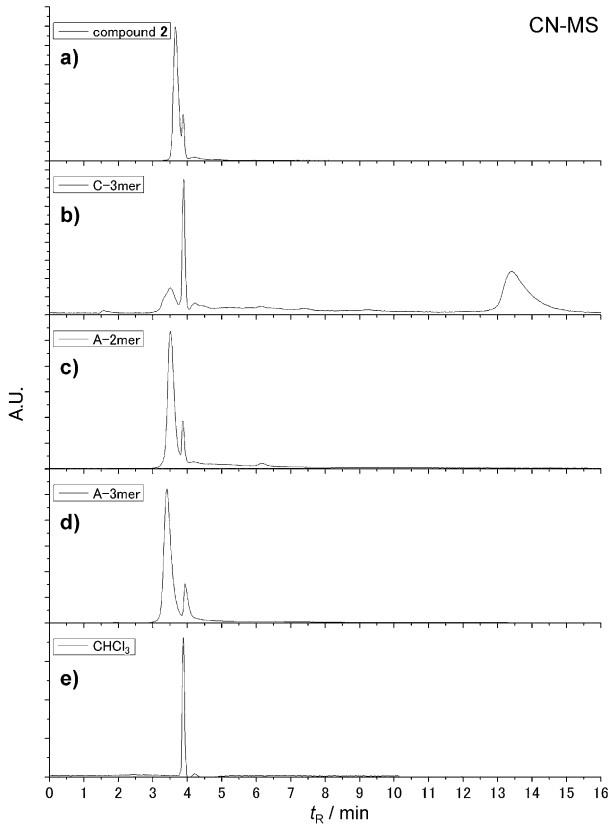

Figure 4. Chromatograms of: a) **2b**, b) C-3mer, c) A-2mer, d) A-3mer, and e) chloroform with analytical HPLC column CN-MS (4.6 mm (ID), 15 cm (length)). A mixture of toluene and pyridine (15:85 v/v) was used as the eluent.

Larger retention factors for C-3mer (ca. 3) were observed with NPE and CN-MS, and the retention factors of $k_{\mathbf{2b}}$ remained

Table 1. Retention factors (k) of compounds on modified silica gel HPLC columns.

Run	Column	Retention factors[a]		
		$k_{\mathbf{2b}}$	k_{CHCl_3}	$k_{\text{C3mer }\mathbf{1b}}$
1	CN-MS	0.08	0.14	2.95
2	C_{18}-MS-II	0.08	0.25	0.04
3	Cholester	0.08	0.24	0.02
4	πNAP	0.08	0.12	0.88
5	PBB-R	0.08	0.10	0.94
6	PYE	0.10	0.10	1.68
7	NPE	0.09	0.14	3.03

[a] $k=(t-t_0)/t_0$; t_0: retention time of A-3mer.

below 0.1. For comparison, TLC analysis was performed with an unmodified SiO_2 plate with a mixture of toluene/pyridine (15:85) as the eluent; in this case, all of the analytes (**2b**, A-2mer, A-3mer, and C-3mer) eluted to the top of the plate (R_f = 1), which indicated that there was almost no interaction of the analytes with the silanol residues in this solvent system. The specific separation mechanism of C-3mer **1b** on some modified silica gel columns is discussed below. After the survey, cyanopropyl-modified silica gel chromatography was selected for use in the more efficient separation of cyclic trimers from the crude reaction mixtures. In Figure 5a and b, chromatograms of the reaction mixtures of the C-3mers synthesized from **2a** and **2b** obtained with a shorter CN-MS column (I.D. = 4.6 mm × 50 mm) are shown. The reaction mixtures are the same samples that were analyzed by using the GPC systems shown in Figure 2a and b, respectively. The peaks occurring at 2.8 and 6 mL in Figure 5a and b, respectively, correspond to the cyclic trimers **1a** and **1b**, respectively. These were eluted much later than most of the other oligomers, even from the crude reaction mixtures. The tailing behavior observed in the ethyl-substituted cyclic trimer **1b** suggests a stronger interaction with cyanopropyl moieties than that with the Mes-substituted cyclic trimer **1a**. The peaks that eluted later than the cyclic trimers, at 4.7 (Figure 5a) and 21 mL (Figure 5b), were assigned to a Mes-substituted monohydrolyzed cyclic trimer (Figures S8 and S9 in the Supporting Information) and an ethyl-substituted cyclic tetramer (Figure S10 in the Supporting Information), respectively, from MALDI-TOF MS analysis. Finally, preparative chromatographic separation of both Mes- and ethyl-substituted cyclic trimers **1a** and **1b** from the corresponding crude reaction mixtures was carried out on silica gel modified with cyanopropyl groups (Cyanogel) purchased from the Yamazen Corporation for flash chromatography. These were purified by Cyanogel chromatography with a mixture of pyridine and toluene (85:15) as the eluent. This purification method was much easier than that for the GPC method. Any cyanopropyl-modified silica gel was reused several times to purify different crude mixtures. After purification by Cyanogel column chromatography, the ethyl-substituted C-3mer **1b** was washed with a 0.3 M aqueous solution of citric acid and then with deionized water in $CHCl_3$. The concentrated organic layer was further purified by using an unmodified SiO_2 column chromatography with $CHCl_3$ and ethyl acetate (5:1) as eluents to give **1b** in a 9.0 % yield. Mes-substituted C-3mer **1a** was further purified by recrystallization from 2-butanone and methanol, after Cyanogel column purification, to give **1a** in 13.1 % yield.

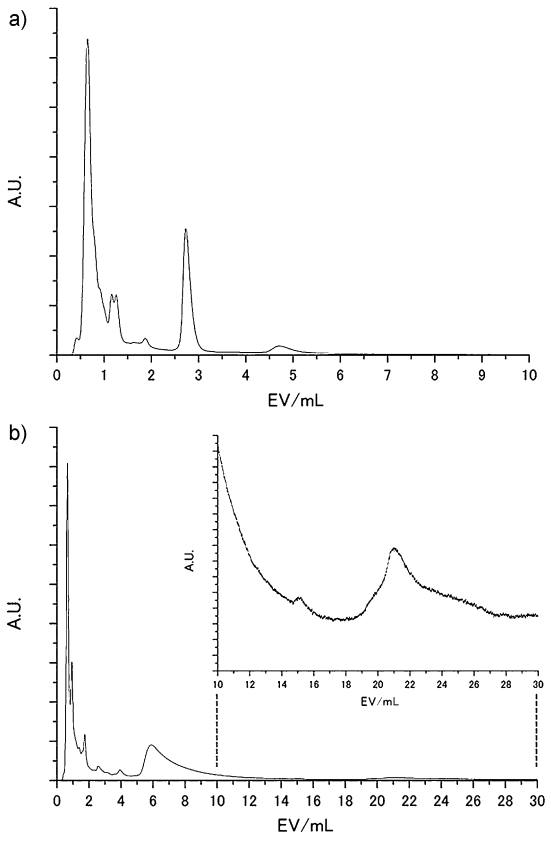

Figure 5. Chromatograms of reaction mixtures obtained by nickel-mediated coupling of: a) **1a**, and b) **1b** by using a Nacalai Tesque 5CN-MS HPLC column ((4.6 mm (ID) × 50 mm (length)), eluent: toluene/pyridine = 15:85 (v/v), flow rate: 0.5 mL min^{-1}, monitored at λ = 556 nm. Peaks at 2.7 mL in a), and 6 mL in b) correspond to **1a** and **1b**, respectively. Inset in b): magnification of the chromatogram from 10 to 30 mL elution volume. The same samples were used in Figures 2a and 5a, and Figures 2b and 5b, respectively.

NMR spectroscopy structural analysis of the C-3mers

NMR spectroscopy structural analysis of cyclic trimers **1a** and **1b** was carried out. The ^{1}H NMR spectra of **1a** and the corresponding monomeric zinc porphyrin **2a** in $CDCl_3$ are shown in Figure 6a and b, respectively.

Similar to the spectrum of **2a**, the spectrum of the C-3mer **1a** showed only a single set of signals, which indicated that **1a** had a D_{3h}-symmetric structure. All of the signals of **1a** could be assigned, as shown in Figure 7, by using 2D NMR spectroscopy techniques: HMQC and HMBC (Figures S11–S14 in the Supporting Information). Similar to the ^{1}H NMR spectrum of **1a**, the spectrum of **1b** also showed simple signals, which indicated that **1b** had a D_{3h}-symmetric structure (Figure S16 in the Supporting Information). In the case of the ^{1}H NMR spectrum of **1b**, coordinated pyridine molecules were observed at δ = 4.3, 3.8, and 2.2 ppm as broad signals. The source of the pyridine molecules was the eluent used in the Cyanogel column chromatography. Because the ^{1}H NMR spectrum of **1b** changed slightly, depending on the amount of pyridine molecules in $CDCl_3$, NMR spectroscopy structural analysis of **1b** was performed in [D_5]pyridine. All 1D and 2D NMR spectroscopy data and assignments of **1b** in [D_5]pyridine are shown in Figures S18–S23 in the Supporting Information. In the case of **1a**, no residual pyridine was observed in the NMR spectra.

X-ray crystallography of C-3mer 1a

An ORTEP model and the molecular structure of C-3mer **1a** are shown in Figure 8 and Figure S24 in the Supporting Information, respectively. A deformed triangular prism shape was observed, in which all six methyl ester groups were directed

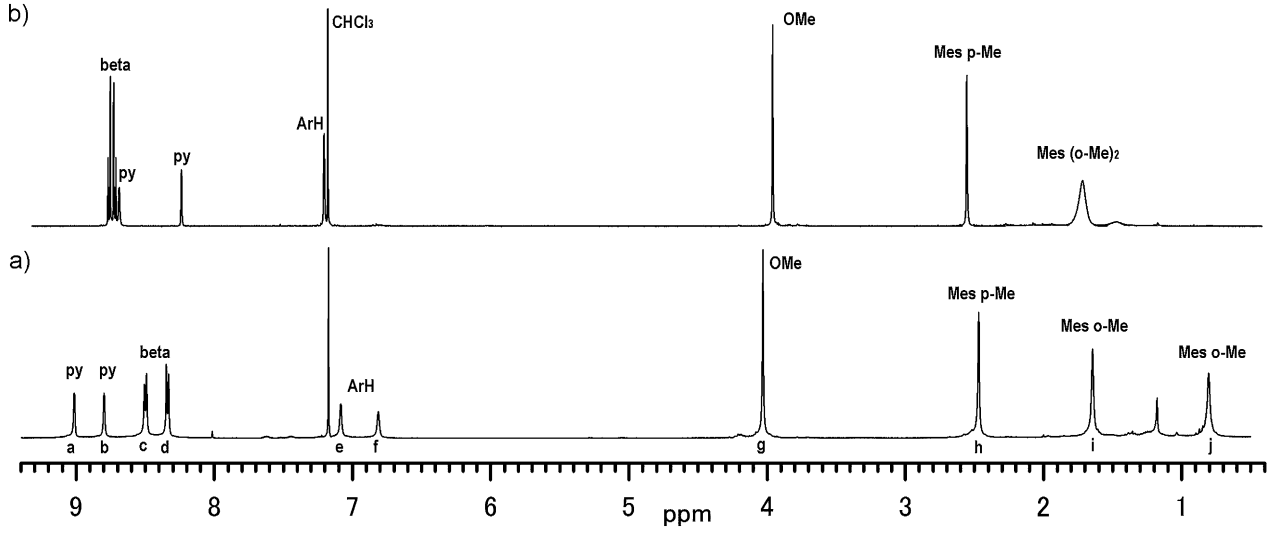

Figure 6. ^{1}H NMR spectra (300 MHz, in $CDCl_3$) of: a) **1 a**, and b) **2 a**. Assignment of signals a–j in spectrum a) correspond to a–j in Figure 7.

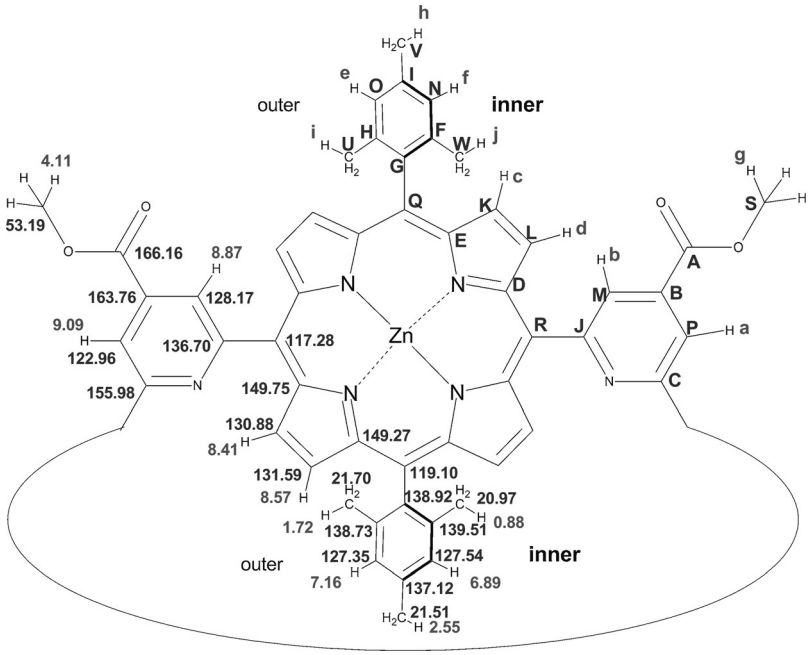

Figure 7. Assignments of ^{1}H (300 MHz) and ^{13}C NMR (75 MHz) signals of cyclic trimer **1 a** in $CDCl_3$.

toward the outside, whereas the nitrogen atoms on the bipyridyl groups were directed toward the inside.

The distance between the two zinc ions was 9.64–9.70 Å (Table 2), which indicated that C-3mer **1 a** had a one-nanometer-sized space inside. Although the D_{3h} symmetry of **1 a** was observed in the ^{1}H NMR data, a C_s-symmetric structure was observed in the crystal structure because of the incline in one of the three porphyrin groups in **1 a**, which allowed it to interact with a bipyridyl moiety in a neighboring cyclic porphyrin **1 a**. The bipyridyl (C(17)–C(21)) and Mes (C(67)–C(69)) moieties on the symmetric plane passing through the Zn(2), C(66), C(70), and C(71) atoms are disordered, as shown in Figure S24 in the Supporting Information.

The angle of the porphyrin plane tilted away from the perpendicular of the mean plane containing the three 2,2′-bpy parts is 31° (Figure 9). This result suggests that, in solution, the porphyrin moiety in **1 a** can rotate approximately ±30° along the axis through the two *meso* positions connected to the two pyridyl parts.

Mechanisms of specific separations of C-3mer on modified silica gel columns

From the chemical structures of the modified columns shown in Figure 3 and the retention factors of C-3mer **1 b** on the columns listed in Table 1, the columns can be classified into three groups. Two columns, C18-MS-II and Cholester, have nonaromatic acyclic and cyclic residues, and they have almost no retention capability for C-3mer **1 b** (< 0.04). These columns are classified as group A. Three columns, PYE, πNAP, and PBB-R, have nonpolar aromatic residues, and their retention capability for C-

Table 2. Zinc center distances [Å] for **1 a**.[a]

Bond	Distance
Zn(1)–Zn(2)	9.6404(12)
Zn(1)–Zn(1)#1	9.7046(16)

[a] Symmetry transformations used to generate equivalent atoms: #1 $x,-y+1/2,z$.

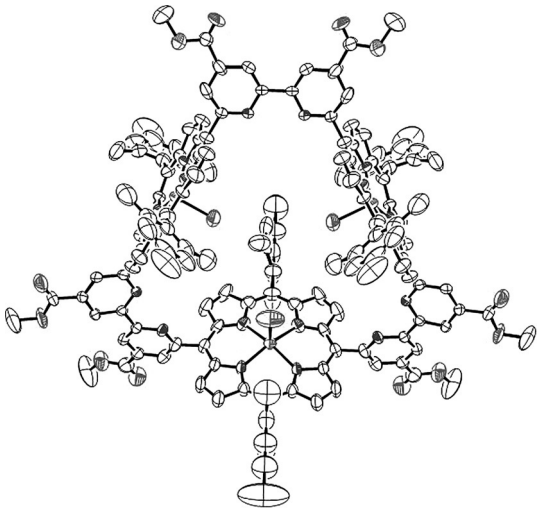

Figure 8. ORTEP drawing of **1a**. Ellipsoids are drawn at the 50 % probability level; hydrogen atoms, coordinated methanol molecules, and disordered moieties were omitted for clarity. Symmetry transformations used to generate equivalent atoms: #1 $x,-y+1/2,z$.

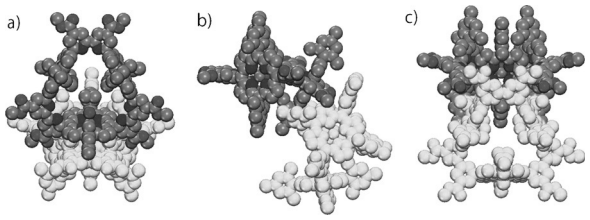

Figure 9. Molecular packing of **1a** observed by X-ray single-crystal analysis; hydrogen atoms are omitted for clarity. A light-colored molecule is an adjacent one (**1a**): a) top view, b) side view, c) front view. The methyl group observed in the center of the C-3mer in a) is disordered at the two carbon positions.

3mer **1b** is moderate (0.88–1.68). These columns are classified as group B. The last two columns, NPE and CN-MS, have polar residues, and they retained C-3mer **1b** the most strongly (ca. 3.0). These columns are classified as group C. Because of the difference in chemical structures between groups B and C, the mechanism of their specific separation was considered to be different.

To discuss these mechanisms, the effect of the solvent eluent was examined. When chloroform was used as an eluent on the NPE column (group C), acyclic ethyl A-3mer and C-3mer **1b** were adsorbed on the column and were not eluted within a retention time (t_R) of 30 min, whereas monomeric **2b** was eluted at $t_R = 4$ min immediately (Figure S25 in the Supporting Information). Increasing the polarity of the eluent by using a toluene/pyridine system on the NPE column caused immediate elution of ethyl A-2mer and ethyl A-3mer, followed by a significantly delayed elution of C-3mer **1b** (Figure S26 in the Supporting Information). These observations are explained by dipole–dipole interactions between nitrobenzene moieties on the NPE column and the functional groups on ethyl A-2mer, ethyl A-3mer, and C-3mer **1b**. Because of the restricted conformation of the 2,2′-bpy groups of the C-3mer, the partial dipole moment must be larger than the 2,2′-bpy groups on ethyl A-2mer and ethyl A-3mer, which can assume different conformations by rotating along the C–C bond between two adjacent pyridyl moieties. Pyridine is considered to be a polar solvent that cancels out the relatively weak dipole–dipole interactions between the nitrobenzene moieties and ethyl A-2mer and ethyl A-3mer, and only strong dipole–dipole interactions with the NPE column for C-3mer **1b** were observed, even in polar pyridine. However, on PYE, chloroform acted in an entirely different manner. Thus, when chloroform was used as an eluent on a PYE column (group B), both ethyl A-3mer and C-3mer **1b** were eluted immediately with slight tailing. The t_R values of the peak maxima were earlier than that of **2b** (Figure S27 in the Supporting Information). The specific retention of C-3mer **1b** on a PYE column was only observed when pyridine was used as an eluent, as shown in Figure S6a in the Supporting Information. This observation suggests that chloroform suppresses any interaction between the pyrenyl groups on the PYE column and C-3mer **1b**, whereas pyridine helps interactions of the PYE column and C-3mer **1b**. To obtain information on the interaction of chloroform with C-3mer **1b**, pyridine-free C-3mer **1b** was prepared by washing with a solution of citric acid several times until any residual pyridine was removed completely.

The ^{1}H NMR spectrum of pyridine-free C-3mer **1b** in $CDCl_3$ exhibited very broad signals, which indicated that conformational isomers existed and that the exchange rate among the isomers was slow on the NMR spectroscopy timescale (Figure S28 in the Supporting Information). The broad signals became sharp with D_{3h} symmetry in the presence of trace amounts of pyridine or when only [D_5]pyridine was used (Figures S16 and S18 in the Supporting Information).

These NMR spectroscopy observations can be explained by the chloroform molecules being held tightly within the C-3mer with several conformational arrangements and the exchange rate among the conformers being slow. A coordinating solvent, such as pyridine, probably increases the rate of conformational exchange by rapid coordination exchange between the ligand and zinc ion and, during this process, the chloroform molecules held within the C-3mer are ejected from the inside.

To represent the chromatographic conditions of a PYE column with pyridine, a ^{1}H NMR spectroscopy titration experiment of C-3mer **1b** in the presence of *N*-methylimidazole (Im) with pyrene was carried out (Figure S29 in the Supporting Information). We used Im instead of pyridine because the association constant of zinc tetraphenylporphyrin is larger ($\log K = 4.66$) than that of pyridine ($\log K = 3.52$)[18], and monitoring the ^{1}H NMR signal of the N-methyl part was applicable.

A mixture of C-3mer **1b** (3.6 mM) and Im (ca. 20 equiv) in $(CDCl_2)_2$ was prepared. Under these conditions, all zinc moieties had to have been coordinated with Im from both the inside and outside of the C-3mer to give five-coordinated Im–zinc porphyrin complexes (B in Figure S29 in the Supporting Information). The ^{1}H NMR spectrum obtained is shown in Figure S30 in the Supporting Information, and a broad signal assigned to the N-methyl group was observed at $\delta = 3.25$ ppm. The chemical shift of the signal maximum of the broad signal

is reasonable because an average signal caused by exchange of one Im molecule coordinated from the inside of the C-3mer, two Im molecules coordinated from the outside of the C-3mer, and about 17 free Im molecules. The chemical shifts of Im molecules coordinated with the outside and inside of the C-3mer were estimated to be $\delta = 2.21$ and -1.3 ppm, respectively, from the complex of monomeric C-3mer **1b** and Im (0.25 equiv) in $(CDCl_2)_2$, and from variable-temperature NMR spectroscopy experiments of C-3mer with Im (0.5 equiv) at $-40\,^{\circ}C$. At room temperature, these coordinating Im molecules exchanged rapidly with free Im molecules, the N-methyl group of which was observed at $\delta = 3.64$ ppm, to give a broad signal at $\delta = 3.25$ ppm as an averaged signal. The addition of pyrene to the mixture caused a downfield shift of the signal, which almost stopped at $\delta = 3.32$ ppm when about 20 equivalents of pyrene had been added to the mixture (Figure S31 in the Supporting Information). The resulting chemical shift is reasonable if three molecules are coordinated on the outside and no Im molecules exist on the inside.

The change in chemical shift of the pyrene molecules added during the titration also caused a downfield shift of the signals from the initial value upon addition of 0.9 equivalents of pyrene, and the signal eventually approached the value of free pyrene (Figure S32 in the Supporting Information). These observations indicate that the pyrene molecules pushed out the Im molecules from inside the C-3mer, and the pyrene molecules then became included inside the C-3mer as a host–guest complex. Based on molecular modeling, only one pyrene molecule can exist in the center of a cavity of C-3mer, and therefore, the observed change in chemical shift suggests that pyrene molecules in the system are exchanged.

Similarly, an NMR spectroscopy titration experiment of C-3mer **1b** with nitrobenzene was also carried out. Although the phenomenon of ejecting Im molecules from inside C-3mer was observed (Figure S33 in the Supporting Information), no inclusion of nitrobenzene in the C-3mer was observed (Figure S34 in the Supporting Information). This result also suggests that the mechanism of specific chromatographic separation of C-3mer on group C columns is different from that on group B columns. The inclusion of nonpolar π aromatic residues on the columns into the C-3mer, and dipole–dipole interactions of polar residues on the columns with the partial dipole moiety of the C-3mer are the most probable mechanisms for group B and C columns, respectively. Used as an eluent, pyridine has a dual role as a coordination ligand and as a polar solvent for each mechanism.

Complexation of the bipyridyl parts in the C-3mer 1a

Complexation of the bipyridyl parts in cyclic trimer **1a** was examined for various metal ions with compounds such as $Ni^{II}Cl_2$ and $Cu^{I}I$, which are employed in fluorescence spectroscopy. The addition of transition-metal ions caused fluorescence quenching from cyclic trimer **1a**, which suggested a heavy-metals effect after complexation of the metal ions with the bipyridyl parts of **1a**. For a more quantitative analysis, titration of **1a** with an η^3-allylpalladium tetrafluoroborate complex was carried out. A solution of η^3-allylpalladium tetrafluoroborate complex in $CHCl_3$ was added portionwise (0.5 equiv each) to a solution of cyclic trimer **1a** (6 equiv) in $CHCl_3$. After stirring for 15 min after each addition, each aliquot was diluted 1000 times to give a solution of about 0.38 μM in chloroform. UV/Vis and fluorescence spectra of the diluted samples were recorded (Figure 10).

In the UV/Vis spectra, the maximum of the Soret band shifted toward the blue, from $\lambda = 425.5$ to 422.5 nm, whereas the maxima of the Q bands shifted toward the red, from $\lambda = 560$ and 606 to 564 and 630 nm, with significant broadening. At the same time, a successive absorption or scattering in the wavelength range from $\lambda = 320$ to 700 nm was observed. In the fluorescence spectra, addition of two equivalents of a palladium complex resulted in almost complete quenching of the fluorescence from **1a**. The mixture of **1a** with an η^3-allylpalladium tetrafluoroborate complex (6 equiv) was analyzed by using ESI-TOF MS and ^1H NMR spectroscopy in $CDCl_3$. From the ESI mass spectrum, the $[\mathbf{1a} + (\text{allylpalladium})_3]_3^+$ species and its derivatives were observed as the dominant ones (Figure S35 in the Supporting Information). By comparing the NMR spectrum

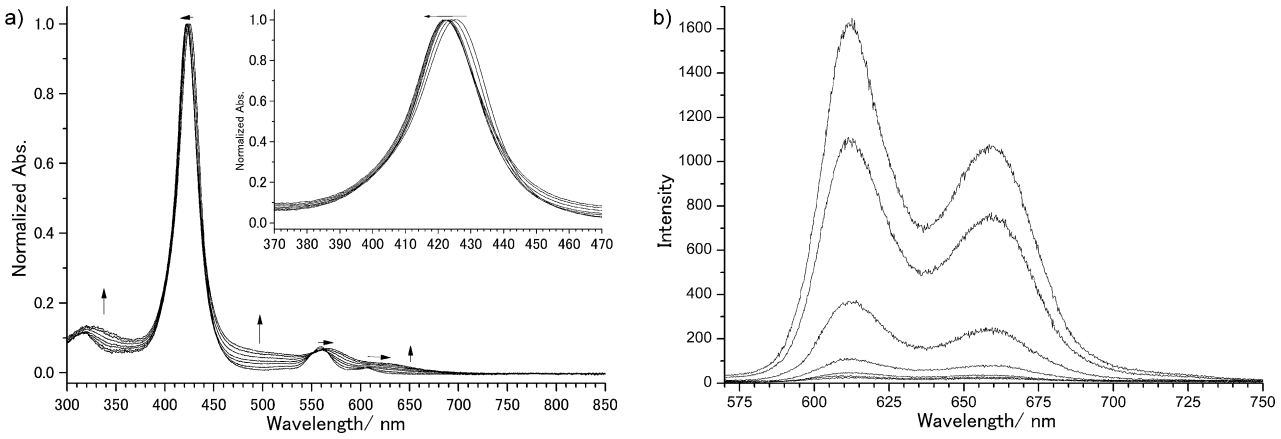

Figure 10. a) UV/Vis spectral changes to **1a** upon addition of an η^3-allylpalladium tetrafluoroborate complex in $CHCl_3$. (Normalized at the peak maxima of their Soret bands $\lambda \approx 425$ nm.) Inset: the expanded spectra from $\lambda = 370$ to 470 nm. b) Fluorescence spectral changes of the same titration of a) excited at $\lambda = 556$ nm. (Their intensities were normalized by being divided with the absorbance at the excited wavelength.)

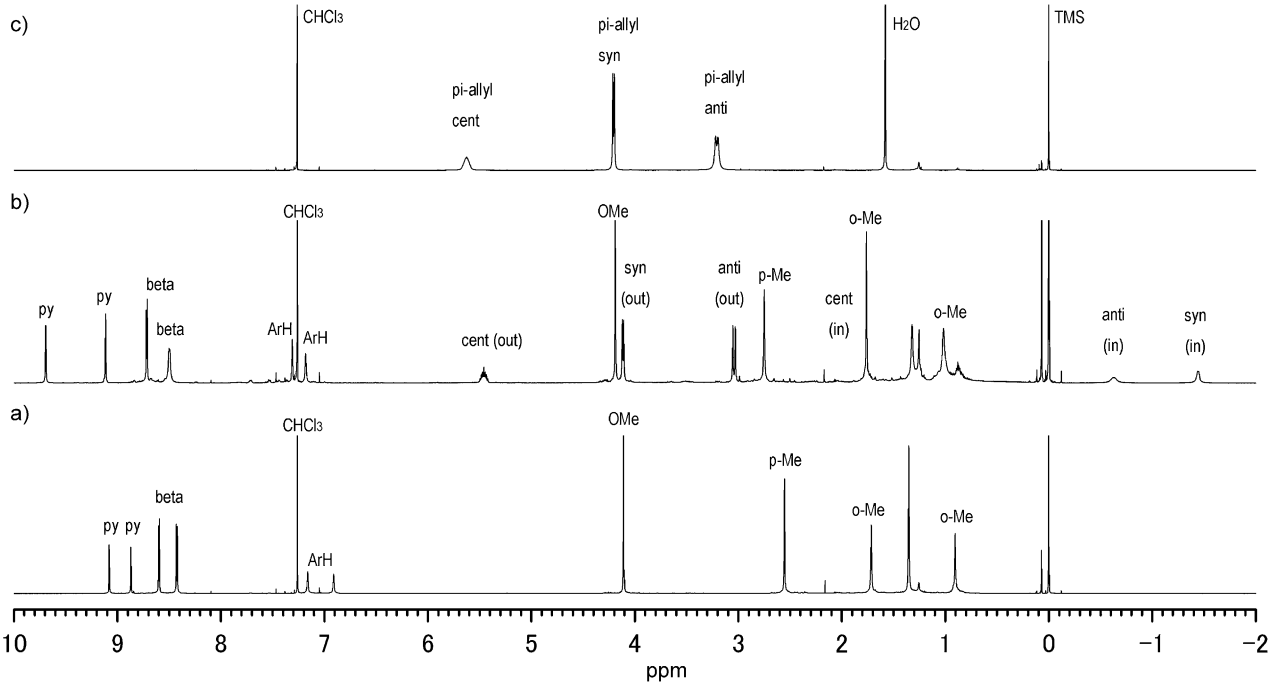

Figure 11. ^{1}H NMR spectra (500 MHz, in $CDCl_3$) of: a) **1a**, b) a mixture of **1a** with η^3-allylpalladium tetrafluoroborate complex (6 equiv), and c) η^3-allylpalladium tetrafluoroborate complex.

of a mixture of **1a** and the η^3-allylpalladium tetrafluoroborate complex (Figure 11b) with reference spectra (Figure 11a and c), characteristic η^3-allylpalladium species were observed at $\delta =$ 1.8, −0.7, and −1.4 ppm, and were considered to be located within the cyclic porphyrin.

Assignment of the allylpalladium species was performed by using the coupling constants in the ^{1}H NMR, ^{1}H–^{1}HCOSY, NOESY, and HMQC spectra, as shown in Figure S36 in the Supporting Information. Both NMR spectroscopy and ESI-MS data clearly show the formation of the [**1a**–$(allylPd)_3$] complex (Scheme 2). These complexation experiments indicate that the three bipyridyl parts can work as bidentate bis(nitrogen) ligands.

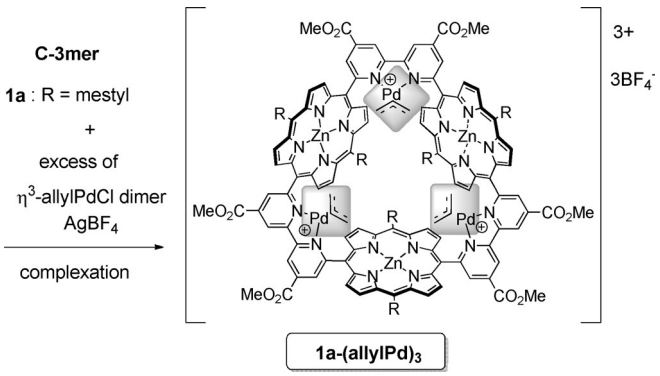

Scheme 2. Complexation of an η^3-allylpalladium complex with C-3mer **1a**.

Demetalation of zinc ions from C-3mer 1a and incorporation of iron(III) ions

To demonstrate that the three tetradentate porphyrinato parts in cyclic trimer **1a** also worked as versatile ligands for multicofacial multimetalloporphyrin complexes, demetalation of the zinc ions from **1a** and incorporation of iron(III) ions was carried out. Iron porphyrins are well known as oxidation catalysts and as a model for cytochrome P450.[19] Treatment of **1a** with trifluoroacetic acid (TFA) and concentrated H_2SO_4 in dry $CHCl_3$ at 0 °C, followed by neutralization with $NaHCO_3$ gave the free-base porphyrin **6a**. The structure of **6a** was confirmed by means of NMR spectroscopy (Figures S37 and S38 in the Supporting Information) and high-resolution MALDI-TOF MS analysis (Figures S39 and S40 in the Supporting Information). The D_{3h}-symmetric structure was observed in the NMR spectrum. Treatment of $[Fe(CO)_5]$ and iodine with **6a** in toluene, followed by ligand exchange with a 1 M solution of HCl, gave corresponding iron(III) C-3mer **7a** (Scheme 3). Structural analysis was performed by UV/Vis spectroscopy and MALDI-TOF MS, as shown in Figures S41 and S42 in the Supporting Information. This observation suggests that the C-3mers **1** are precursors for cyclic tris(metallo)porphyrin derivatives.

Conclusion

The one-step synthesis of D_{3h}-symmetric cyclic porphyrin trimers **1** was achieved from a nickel-mediated reductive coupling of bis(chloropyridyl)porphyrinatozinc **2**. Although cyclic trimers **1** were obtained as a mixture that contained other cyclic and acyclic porphyrin oligomers, cyclic trimers **1** could

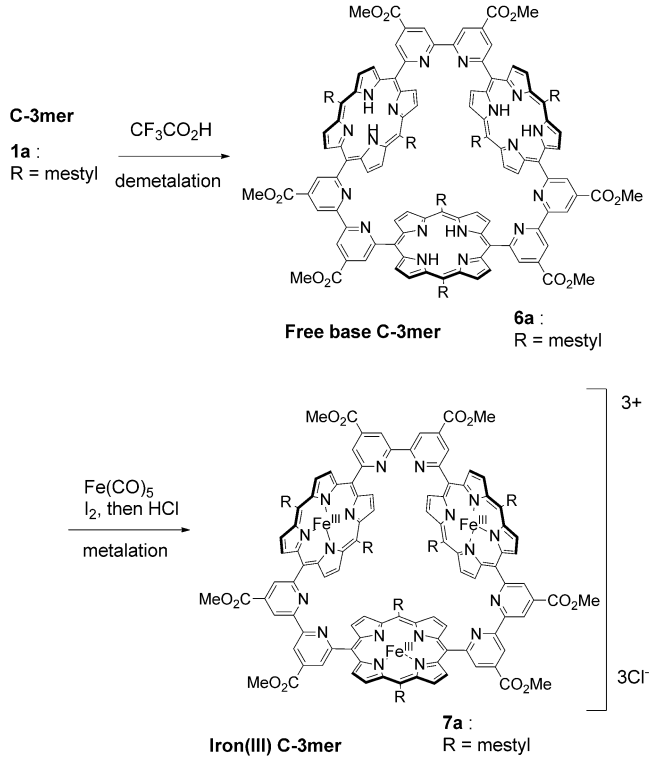

Scheme 3. Demetalation of **1a** (R = Mes) into free-base C-3mer **6a** and incorporation of iron(III) ion into **6a** to give iron(III) C-3mer **7a**.

be isolated efficiently from the mixtures by using cyanopropyl-modified silica gel column chromatography. Structural analysis of cyclic trimers **1** was carried out by using NMR spectroscopy and X-ray crystallography. As a result, in solution, the cyclic trimers were found to assume an apparent D_{3h}-symmetric macrocyclic structure, in which three bipyridyl parts were directed toward the center and six carboxylic ester groups existed outside the ring. Treatment of an η^3-allylpalladium complex with cyclic trimer **1a** gave tris(palladium) complex **1a**–$(allylPd)_3$, which indicated that the bipyridyl moieties inside the ring could work as bidentate metalloligands. The zinc porphyrin parts also worked as tetradentate metallo ligands of an iron porphyrin complex after acidic demetalation of the zinc ions. These demonstrations show that cyclic trimers **1** are versatile macrocyclic ligands for multicofacial multimetallic complexes. Unique catalytic activity for multimetallic sites within the restricted approximately one-nanometer-sized space is expected.

From the effect of the solvents chloroform and pyridine on PYE columns and the results from NMR spectroscopy titration experiments of C-3mer **1b** with pyrene, the following interesting relationship between chloroform, pyridine, and pyrene in C-3mer was revealed. Although pyrene molecules alone could not push out chloroform molecules held in C-3mer, this became possible with the assistance of a coordinating solvent, such as pyridine. The coordination of pyridine with zinc ions in the C-3mer overcame the interaction of chloroform molecules inside the C-3mer, and the exchange rate of the coordination bond between the inner and outer moieties was rapid. Then, pyrene molecules could be inserted inside the C-3mer. Such a cooperative effect to form a host–guest complex is unique. The two different separation mechanisms for C-3mer observed for group B and C columns will be applicable for the isolation of other macrocyclic compounds, and a combination of methods will allow new strategies to be pursued to prepare various macrocycles.

Experimental Section

Synthesis of 1a

$[Ni(cod)_2]$ (174 mg, 0.63 mmol) and 2,2′-bpy (101 mg, 0.65 mmol) were placed in a 200 mL of Schlenk flask under a flow of Ar. Dry DMF (60 mL) was added to the mixture, and the mixture was stirred for 5 min at 25 °C to give a dark-purple solution. Porphyrinatozinc **2a** (30.7 mg, 0.032 mmol) and dry DMF (29 mL) were added to the mixture and stirred under argon for 16 h at 50 °C. $CHCl_3$ (20 mL) was added to the mixture, which was washed with an aqueous solution of citric acid (0.3 M, 80 mL) four times. Subsequently, the organic layer was washed with an aqueous solution of NH_4OH (25 %, 20 mL) three times. The organic layer was filtered through a membrane filter (Omnipore, 0.1 μm), and the filtrate was concentrated to give a purple solid (33.3 mg). The crude mixture was purified by Cyanogel (Yamazen YFLC Gel, 40 μm dp, 60 Å pore) column chromatography with a mixture of toluene and pyridine (15:85 v/v) as the eluent to give **1a** (5.5 mg). This sample was recrystallized from 2-butanone and methanol to afford pure **1a** (3.7 mg, 13.1 %). All of the ^1H and ^{13}C NMR signals in $CDCl_3$ were assigned as shown in Figure 7. The 1D and 2D NMR data are shown in Figure 6 and Figures S11–S14 in the Supporting Information. MALDI-TOF-MS (dithranol): *m/z* calcd for $[C_{156}H_{120}N_{18}O_{12}Zn_3 + Na]^+$ $[M + Na]^+$: 2651.7100; found: 2651.7112 (Figure S15 in the Supporting Information); UV/Vis (pyridine): λ_{max} (ε) = 432.2 (7.0×10^5), 564.2 (4.3×10^4), 610.2 nm (1.3×10^4 M^{-1} cm^{-1}).

Allylpalladium complex 1a–$(allylPd)_3$

A stock solution of η^3-allylpalladium tetrafluoroborate complex was prepared from η^3-allylpalladium chloride dimer (3.9 mg, 11 μmol) and silver tetrafluoroborate (7.3 mg, 37 μmol) in chloroform (1.0 mL) at 0 °C. This stock solution was added portionwise (0.5 equiv each up to 6 equiv) to a solution of **1a** (1.0 mg, 0.38 μmol) in degassed $CHCl_3$ (1.0 mL). After 15 min of stirring for each addition, each aliquot was diluted 1000 times to give a solution of approximately 0.38 μM in chloroform. UV/Vis and fluorescence spectra of the diluted sample were collected (see text and Figure 10). A mixture of **1a** and η^3-allylpalladium tetrafluoroborate complex (6 equiv) was analyzed by ESI-MS and ^1H NMR spectroscopy (see text and Figure 11 b and Figure S35 in the Supporting Information).

Demetalation of zinc porphyrin 1a to free-base porphyrin 6a

TFA (2.0 mL) was added dropwise to a solution of **1a** (5.0 mg) in dry chloroform (2.0 mL) at 0 °C to give a green solution. Subsequently, concentrated H_2SO_4 (0.2 mL) was added dropwise to give a pale-brown suspension. The reaction mixture was added to a saturated solution of $NaHCO_3$ to maintain pH 8–9. The organic layer was extracted with chloroform, dried over anhydrous Na_2SO_4, and concentrated under reduced pressure. The residue was purified by flash column chromatography on a short SiO_2 column to give free-base C-3mer **6a** (4.0 mg) as a brown solid. ^1H NMR (300 MHz,

$CDCl_3$): $\delta = 9.09$ (d, 2H, $J = 1.4$ Hz), 8.87 (d, 2H, $J = 1.4$ Hz), 8.57 (d, 4H, $J = 4.6$ Hz), 8.36 (d, 4H, $J = 4.6$ Hz), 7.07 (br s, 2H), 6.85 (br s, 2H), 4.13 (s, 6H), 2.55 (s, 6H), 1.73 (s, 6H), 1.01 (s, 6H), −3.17 ppm (s, 2H); ^{13}C NMR (75 MHz, $CDCl_3$): $\delta = 166.1$ (C=O), 162.9 (C), 156.5 (C), 139 (broad), 138.3 (C), 137.4 (C), 136.9 (C), 131 (broad), 128.5 (CH), 127.6 (CH), 121.1 (CH), 118.3 (C), 116.9 (C), 53.2 (CH_3), 21.5 ppm (CH_3); MALDI-TOF-MS (dithranol): *m/z* calcd for $[C_{156}H_{126}N_{18}O_{12}+H]^+$, $[C_{156}H_{126}N_{18}O_{12}+Na]^+$: 2443.9875, 2465.9695; found: 2443.9812 $[M+H]^+$, 2465.9697 $[M+Na]^+$; UV/Vis ($CHCl_3$): $\lambda_{max} = 419.9$, 516.5, 591.4, 647.5 nm.

Synthesis of iron(III) porphyrin 7a

Excess I_2 (76.5 mg) was added to a solution of **6a** (6.5 mg, 2.7 μmol) in toluene (10.0 mL) under Ar. To the mixture, an excess of $[Fe(CO)_5]$ (40 μL) was added. After 5 min of stirring at RT, the mixture was heated at 60 °C for 1 h under an Ar atmosphere. At 0 °C, a 1 M solution of HCl was added to the mixture, and the mixture was stirred for 5 min. The organic layer was washed with distilled water and brine, dried over anhydrous Na_2SO_4, and concentrated under reduced pressure to give **7a** (6.7 mg). This sample was analyzed by MALDI-TOF MS and UV/Vis spectroscopy, as shown in Figures S42 and S43 and Figure S41 in the Supporting Information, respectively. UV/Vis ($CHCl_3$): λ_{max} (Abs) = 380.0 (0.270), 420.2 (0.435), 515.0 (0.077), 580.0 (0.026), 670.0 nm (0.014).

Acknowledgements

A.S. acknowledges financial support by KAKENHI (24510140) from the Japan Society for the Promotion of Science (JSPS).

Keywords: column chromatography · macrocycles · multinuclear complex · porphyrinoids · synthesis design

[1] a) L. G. Mackay, R. S. Wylie, J. K. M. Sanders, *J. Am. Chem. Soc.* **1994**, *116*, 3141 – 3142; b) M. Marty, Z. Clyde-Watson, L. J. Twyman, M. Nakash, J. K. M. Sanders, *Chem. Commun.* **1998**, 2265 – 2266; c) M. Yoshizawa, T. Kusukawa, M. Fujita, K. Yamaguchi, *J. Am. Chem. Soc.* **2000**, *122*, 6311 – 6312; d) M. L. Merlau, M. del Pilar Mejia, S. T. Nguyen, J. T. Hupp, *Angew. Chem. Int. Ed.* **2001**, *40*, 4239 – 4242; *Angew. Chem.* **2001**, *113*, 4369 – 4372; e) M. Yoshizawa, T. Kusukawa, M. Fujita, S. Sakamoto, K. Yamaguchi, *J. Am. Chem. Soc.* **2001**, *123*, 10454 – 10459; f) P. Thordarson, E. J. A. Bijsterveld, A. E. Rowan, R. J. M. Nolte, *Nature* **2003**, *424*, 915 – 918; g) D. Fiedler, D. H. Leung, R. G. Bergman, K. N. Raymond, *Acc. Chem. Res.* **2005**, *38*, 349 – 358; h) D. Fiedler, R. G. Bergman, K. N. Raymond, *Angew. Chem. Int. Ed.* **2004**, *43*, 6748 – 6751; *Angew. Chem.* **2004**, *116*, 6916 – 6919; i) D. M. Vriezema, M. Comellas Aragonès, J. A. A. W. Elemans, J. J. L. M. Cornelissen, A. E. Rowan, R. J. M. Nolte, *Chem. Rev.* **2005**, *105*, 1445 – 1490; j) M. Kuil, T. Soltner, P. W. N. M. van Leeuwen, J. N. H. Reek, *J. Am. Chem. Soc.* **2006**, *128*, 11344 – 11345; k) S. Jonsson, F. G. J. Odille, P.-O. Norrby, K. Warnmark, *Org. Biomol. Chem.* **2006**, *4*, 1927 – 1948; l) M. D. Pluth, R. G. Bergman, K. N. Raymond, *Science* **2007**, *316*, 85 – 88; m) S. J. Lee, K. L. Mulfort, X. Zuo, A. J. Goshe, P. J. Wesson, S. T. Nguyen, J. T. Hupp, D. M. Tiede, *J. Am. Chem. Soc.* **2008**, *130*, 836 – 838; n) S. J. Lee, S.-H. Cho, K. L. Mulfort, D. M. Tiede, J. T. Hupp, S. T. Nguyen, *J. Am. Chem. Soc.* **2008**, *130*, 16828 – 16829; o) M. Yoshizawa, J. K. Klosterman, M. Fujita, *Angew. Chem. Int. Ed.* **2009**, *48*, 3418 – 3438; *Angew. Chem.* **2009**, *121*, 3470 – 3490; p) K. Oisaki, Q. Li, H. Furukawa, A. U. Czaja, O. M. Yaghi, *J. Am. Chem. Soc.* **2010**, *132*, 9262 – 9264; q) T. Murase, M. Fujita, *Chem. Rec.* **2010**, *10*, 342 – 347; r) T. R. Cook, Y.-R. Zheng, P. J. Stang, *Chem. Rev.* **2013**, *113*, 734 – 777; s) H. Amouri, C. Desmarets, J. Moussa, *Chem. Rev.* **2012**, *112*, 2015 – 2041; t) M. Guitet, P. Zhang, F. Marcelo, C. Tugny, J. Jiménez-Barbero, O. Buriez, C. Amatore, V. Mouriès-Mansuy, J.-P. Goddard, L. Fensterbank, Y. Zhang, S. Roland, M. Ménand, M. Sollogoub, *Angew. Chem. Int. Ed.* **2013**, *52*, 7213 – 7218; *Angew. Chem.* **2013**, *125*, 7354 – 7359; u) J. Hong, K. E. Djernes, I. Lee, R. J. Hooley, F. Zaera, *ACS Catal.* **2013**, *3*, 2154 – 2157; v) J. Liu, L. Chen, H. Cui, J. Zhang, L. Zhang, C.-Y. Su, *Chem. Soc. Rev.* **2014**, *43*, 6011 – 6061; w) C. Zhao, F. D. Toste, K. N. Raymond, R. G. Bergman, *J. Am. Chem. Soc.* **2014**, *136*, 14409 – 14412.

[2] a) R. D. Adams, F. A. Cotton, *Catalysis by Di- and Polynuclear Metal Cluster Complexes*, Wiley, New York, **1998**; b) N. C. Gianneschi, P. A. Bertin, S. T. Nguyen, C. A. Mirkin, L. N. Zakharov, A. L. Rheingold, *J. Am. Chem. Soc.* **2003**, *125*, 10508 – 10509; c) N. Tsukada, S. Ninomiya, Y. Aoyama, Y. Inoue, *Pure Appl. Chem.* **2008**, *80*, 1161 – 1166; d) X. Liu, W. Chen, *Organometallics* **2012**, *31*, 6614 – 6622; e) S. Takano, D. Takeuchi, K. Osakada, N. Akamatsu, A. Shishido, *Angew. Chem. Int. Ed.* **2014**, *53*, 9246 – 9250; *Angew. Chem.* **2014**, *126*, 9400 – 9404.

[3] a) S. J. Lee, A. Hu, W. Lin, *J. Am. Chem. Soc.* **2002**, *124*, 12948 – 12949; b) A. M. Appel, J. E. Bercaw, A. B. Bocarsly, H. Dobbek, D. L. DuBois, M. Dupuis, J. G. Ferry, E. Fujita, R. Hille, P. J. A. Kenis, C. A. Kerfeld, R. H. Morris, C. H. F. Peden, A. R. Portis, S. W. Ragsdale, T. B. Rauchfuss, J. N. H. Reek, L. C. Seefeldt, R. K. Thauer, G. L. Waldrop, *Chem. Rev.* **2013**, *113*, 6621 – 6658; c) P. Buchwalter, J. Rosé, P. Braunstein, *Chem. Rev.* **2014**, *115*, 28 – 126.

[4] a) A. Kless, C. Lefeber, A. Spannenberg, R. Kempe, W. Baumann, J. Holz, A. Börner, *Tetrahedron* **1996**, *52*, 14599 – 14606; b) Q. F. Mokuolu, P. A. Duckmanton, P. B. Hitchcock, C. Wilson, A. J. Blake, L. Shukla, J. B. Love, *Dalton Trans.* **2004**, 1960 – 1970.

[5] a) X. Sun, D. W. Johnson, D. L. Caulder, R. E. Powers, K. N. Raymond, E. H. Wong, *Angew. Chem. Int. Ed.* **1999**, *38*, 1303 – 1307; *Angew. Chem.* **1999**, *111*, 1386 – 1390; b) S. Abe, J. Niemeyer, M. Abe, Y. Takezawa, T. Ueno, T. Hikage, G. Erker, Y. Watanabe, *J. Am. Chem. Soc.* **2008**, *130*, 10512 – 10514; c) J. Moussa, H. Amouri, *Angew. Chem. Int. Ed.* **2008**, *47*, 1372 – 1380; *Angew. Chem.* **2008**, *120*, 1392 – 1400; d) R. Maity, A. Rit, C. Schulte to Brinke, C. G. Daniliuc, F. E. Hahn, *Chem. Commun.* **2013**, *49*, 1011 – 1013.

[6] a) Z. Clyde-Watson, A. Vidal-Ferran, L. J. Twyman, C. J. Walter, D. W. J. McCallien, S. Fanni, N. Bampos, R. Stephen Wylie, J. K. M. Sanders, *New J. Chem.* **1998**, *22*, 493 – 502; b) R. Gramage-Doria, D. Armspach, D. Matt, *Coord. Chem. Rev.* **2013**, *257*, 776 – 816; c) T. Nabeshima, M. Yamamura, *Pure Appl. Chem.* **2013**, *85*, 763 – 776; d) K. Omoto, S. Tashiro, M. Kuritani, M. Shionoya, *J. Am. Chem. Soc.* **2014**, *136*, 17946 – 17949.

[7] a) J. E. Hutchison, T. A. Postlethwaite, C.-h. Chen, K. W. Hathcock, R. S. Ingram, W. Ou, R. W. Linton, R. W. Murray, D. A. Tyvoll, L. L. Chng, J. P. Collman, *Langmuir* **1997**, *13*, 2143 – 2148; b) C. J. Chang, Y. Deng, A. F. Heyduk, C. K. Chang, D. G. Nocera, *Inorg. Chem.* **2000**, *39*, 959 – 966; c) S. Faure, C. Stern, R. Guilard, P. D. Harvey, *J. Am. Chem. Soc.* **2004**, *126*, 1253 – 1261; d) P. Peljo, L. Murtomäki, T. Kallio, H.-J. Xu, M. Meyer, C. P. Gros, J.-M. Barbe, H. H. Girault, K. Laasonen, K. Kontturi, *J. Am. Chem. Soc.* **2012**, *134*, 5974 – 5984.

[8] S. Durot, J. Taesch, V. Heitz, *Chem. Rev.* **2014**, *114*, 8542 – 8578.

[9] a) C. N. Hunter, F. Daldal, M. C. Thurnauer, J. T. Beatty, in *The Purple Phototrophic Bacteria, Series: Advances in Photosynthesis and Respiration, Vol. 28*, Springer, Dordrecht, **2009**; b) N. Aratani, D. Kim, A. Osuka, *Acc. Chem. Res.* **2009**, *42*, 1922 – 1934; c) A. Satake, in *Handbook of Porphyrins: Chemistry, Properties and Applications* (Eds.: A. Kaibara, G. Matsumara) Nova Science Publishers, **2012**, pp. 409 – 428; d) P. Parkinson, C. E. I. Knappke, N. Kamonsutthipaijit, K. Sirithip, J. D. Matichak, H. L. Anderson, L. M. Herz, *J. Am. Chem. Soc.* **2014**, *136*, 8217 – 8220.

[10] a) H. L. Anderson, J. K. M. Sanders, *J. Chem. Soc. Chem. Commun.* **1989**, 1714 – 1715; b) J. K. M. Sanders, in *Comprehensive Supramolecular Chemistry, Vol. 9* (Eds.: J.-P. Sauvage, M. W. Hosseini), Elsevier, Oxford, **1996**, pp. 131 – 164; c) A. L. Kieran, A. D. Bond, A. M. Belenguer, J. K. M. Sanders, *Chem. Commun.* **2003**, 2674 – 2675; d) J. X. Song, N. Aratani, H. Shinokubo, A. Osuka, *J. Am. Chem. Soc.* **2010**, *132*, 16356 – 16357; e) G. n. Gil-Ramírez, S. D. Karlen, A. Shundo, K. Porfyrakis, Y. Ito, G. A. D. Briggs, J. J. L. Morton, H. L. Anderson, *Org. Lett.* **2010**, *12*, 3544 – 3547.

[11] A. Satake, M. Yamamura, M. Oda, Y. Kobuke, *J. Am. Chem. Soc.* **2008**, *130*, 6314 – 6315.

[12] a) O. Mongin, A. Schuwey, M. A. Vallot, A. Gossauer, *Tetrahedron Lett.* **1999**, *40*, 8347 – 8350; b) T. Hori, N. Aratani, A. Takagi, T. Matsumoto, T. Kawai, M. C. Yoon, Z. S. Yoon, S. Cho, D. Kim, A. Osuka, *Chem. Eur. J.* **2006**, *12*, 1319 – 1327; c) M. Hoffmann, C. J. Wilson, B. Odell, H. L. Anderson, *Angew. Chem. Int. Ed.* **2007**, *46*, 3122 – 3125; *Angew. Chem.* **2007**, *119*, 3183 – 3186.

[13] a) J. Z. Li, A. Ambroise, S. I. Yang, J. R. Diers, J. Seth, C. R. Wack, D. F. Bocian, D. Holten, J. S. Lindsey, *J. Am. Chem. Soc.* **1999**, *121*, 8927 – 8940; b) C. Ikeda, A. Satake, Y. Kobuke, *Org. Lett.* **2003**, *5*, 4935 – 4938; c) A. Kato, K. Sugiura, H. Miyasaka, H. Tanaka, T. Kawai, M. Sugimoto, M. Yamashita, *Chem. Lett.* **2004**, *33*, 578 – 579; d) S. Rucareanu, A. Schuwey, A. Gossauer, *J. Am. Chem. Soc.* **2006**, *128*, 3396 – 3413; e) S.-i. Sasaki, H. Tamiaki, *Tetrahedron Lett.* **2006**, *47*, 4965 – 4968; f) M. Hoffmann, J. Kärnbratt, M.-H. Chang, L. M. Herz, B. Albinsson, H. L. Anderson, *Angew. Chem. Int. Ed.* **2008**, *47*, 4993 – 4996; *Angew. Chem.* **2008**, *120*, 5071 – 5074; g) E. Scamporrino, P. Mineo, D. Vitalini, *Tetrahedron* **2011**, *67*, 3705 – 3713.

[14] a) O. Shoji, S. Okada, A. Satake, Y. Kobuke, *J. Am. Chem. Soc.* **2005**, *127*, 2201 – 2210; b) H. Jiang, W. Lin, *J. Am. Chem. Soc.* **2006**, *128*, 11286 – 11297; c) Y. Kuramochi, A. Satake, M. Itou, K. Ogawa, Y. Araki, O. Ito, Y. Kobuke, *Chem. Eur. J.* **2008**, *14*, 2827 – 2841; d) T. Hori, X. Peng, N. Aratani, A. Takagi, T. Matsumoto, T. Kawai, Z. S. Yoon, M.-C. Yoon, J. Yang, D. Kim, A. Osuka, *Chem. Eur. J.* **2008**, *14*, 582 – 595.

[15] a) Y. Tomohiro, A. Satake, Y. Kobuke, *J. Org. Chem.* **2001**, *66*, 8442 – 8446; b) H. Kitagishi, A. Satake, Y. Kobuke, *Inorg. Chem.* **2004**, *43*, 3394 – 3405; c) S. Fukuda, A. Satake, Y. Kobuke, *Thin Solid Films* **2006**, *499*, 263 – 268.

[16] T. Yamamoto, S. Wakabayashi, K. Osakada, *J. Organomet. Chem.* **1992**, *428*, 223 – 237.

[17] L. R. Snyder, *J. Chromatogr. A* **1974**, *92*, 223 – 230.

[18] H. Imai, S. Nakagawa, E. Kyuno, *J. Am. Chem. Soc.* **1992**, *114*, 6719 – 6723.

[19] a) K. S. Suslick, in *The Porphyrin Handbook, Vol. 4* (Eds.: K. M. Kadish, K. M. Smith, R. Guilard) Academic Press, New York, **2000**, pp. 41 – 63; b) J. T. Groves, K. Shalyaev, J. Lee, in *The Porphyrin Handbook, Vol. 4* (Eds.: K. M. Kadish, K. M. Smith, R. Guilard), Academic Press, New York, **2000**, pp. 17 – 40; c) F. A. Walker, U. Simonis, in *Encyclopedia of Inorganic and Bioinorganic Chemistry*, Wiley, New York, **2011**.

Received: May 12, 2015
Published online on July 14, 2015